PCCP

Accepted Manuscript

ROYAL SOCIETY OF CHEMISTRY

www.rsc.org/pccp

Physical Chemistry Chemical Physics

Dynamic Article Links ►

Cite this: DOI: 10.1039/c0xx00000x

PAPER

www.rsc.org/xxxxxx

Bio-Inspired Fabrication of Hierarchical Ni-Fe-P coated Skin Collagen Fiber for the High-Performance Microwave Absorption

Xiaoling Wang[a] Xuepin Liao*[,a,b] Wenhua Zhang[b] Bi Shi*[,a,b]

Received (in XXX, XXX) Xth XXXXXXXXX 20XX, Accepted Xth XXXXXXXXX 20XX

DOI: 10.1039/b000000x

Table of contents entry: Skin collagen fibers (CF) were employed as bio-inspired for the fabrication of high-performance microwave absorption materials. To enhance the microwave absorption of CF, the CF with well defined hierarchical 3D fibrous were coated by Ni-Fe-P coating.

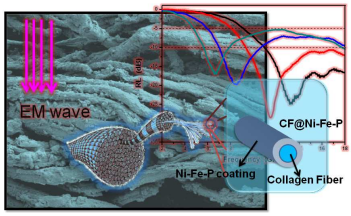

In present investigation, skin collagen fibers (CF) with well defined hierarchical 3D-fibrous structure were employed as bio-inspired for the fabrication of high-performance microwave absorption materials. The hierarchical 3D structure of CF was retained in CF@Ni-Fe-P composites, and the formation of Ni-Fe-P coating on the CF surface was identified by XRD and XPS analysis. Based on the electromagnetism parameters measurements, the maximum reflection loss (RL) of the CF@Ni-Fe-P reached -31.0 dB, and the width of the absorption band which reflection loss values exceeded -10.0 dB covered the whole Ku-band and some part of the X-band (9.5~18.0 GHz). The complex permittivity and complex permeability determination indicated that the electronic loss and magnetic loss were involved in the CF@Ni-Fe-P composites for the microwave absorption. In addition, owning to the magnetic properties of Ni-Fe-P coating, these CF@Ni-Fe-P composites exhibited excellent magnetic characteristic with high saturation magnetization and low coercivity. The present investigation indicated a new possibility for the bio-matrix-based fabrication of high-performance microwave absorbing materials with lightweight and efficient absorption.

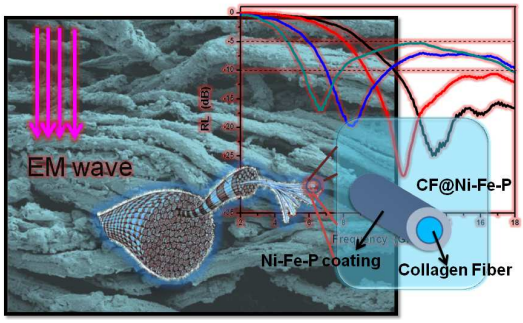

Introduction

With the rapid development of electronic information technology, the electromagnetic (EM) radiation is becoming more and more dense and messy in our living space.[1,2] The problem of powerfully electromagnetic interference (EMI) becomes increasingly serious, which has been one of the most serious pollution problems in modern world. Therefore, the development of high-performance microwave absorption materials which are featured with lightweight, low-cost, flexible and efficient absorption properties is one of the most difficult challenges toward the information technology powered society as a long-term solution for electromagnetic interference (EMI) in near future.[3,4] Conventional microwave absorption materials, such as magnetic ferrites, ultrafine metal powder and conductive fibers, usually have a heavy weight and severe synthesis condition, which impose restrictions on the practical application.[5] On the other hand, even some newly developed microwave absorption materials exhibit high capacity for microwave absorption, such as graphene[6], carbon nano-fibers (CNFs)[7] and conductive polymer composites[8], but the fabrication of these materials often involves complex processes and high cost, which are not applicable for large-scale.[9]

Compared with monolithic absorbing counterparts, the absorbing materials with hierarchical structures have more complicated interfaces, which lead to the dielectric loss properties[10] and form a unique multiple scattering absorption

characteristics. As a result, the hierarchical structures is helpful for improving the microwave absorption performance of absorbing materials.[11] It was found that some natural biomass with hierarchical structure, such as rice-husk, have been used for the fabrication of microwave absorbing materials.[12] This bio-inspired strategy is a facile and elegant method for the fabrication of advanced absorbing materials with well-defined and sophisticated hierarchical structures.

Recently, we reported a serials of high-performance microwave absorption materials based on the skin collagen fiber (CF).[13,14] CF is one of the most abundant renewable animal biomass in nature, which mainly comes from the skin of high-ranking vertebrate. It was proved that these novel CF composites with hierarchical inter-textural structure exhibited excellent lightweight and frequency-tuneable absorption properties. Due to the staggered arrangement of collagen molecules, the multiple reflections of microwave in the hierarchical CF may take place, which significantly enhanced the microwave absorption ability of CF based composites.[13] Furthermore, it has been shown that at least 12% (wt %) structure-participated water is contained in the CF.[15] These structure-participated water molecules can efficiently dissipate the thermal energy transformed from the absorbed microwave, suggesting that the temperature of CF based composites will not increased dramatically under irradiation of microwave, which is beneficial for the reduction of their infrared emitting ability.[14]

According to the transmission line theory, the performance of microwave absorption mainly depends on the intrinsic electrical conductivity, dielectric constant, and magnetic permeability.[16] In terms of these criteria, the dielectric loss and magnetic loss of absorption materials is greatly related with the absorption performance of absorption materials. Our study found that the previous reported CF-based microwave materials only have significant electrical dielectric loss for microwave energy absorption. Therefore, to enhance the advantages of hierarchical structures, a strategy with both dielectric loss and magnetic loss for microwave has been devised for the design of CF-based microwave absorption materials. In our previous report, we have investigated the microwave absorption properties of noble metal (Ag) nanopaticles-embedded CF, which exhibited dielectric loss-type microwave absorption ability in the frequency of 2.0~12.0 GHz (S-band, C-band and X-band).[14] As successive work in the present investigation, we attempted to coat low-cost magnetic metal on CF surface instead of expensive noble metal, and improved the microwave absorbing ability in the whole frequency of 2.0~18.0 GHz, including S-band, C-band, X-band and Ku-band.

In fact, Ni-Fe-P coating has been widely used as soft magnetic materials due to their low coercitity, high permeability and saturation magnetization.[17,18] For the Ni-Fe-P coating, the Fe bulk have higher magnetic property than the Ni bulk, and the Ni atom in the Fe bulk can increase the effective anisotropy field, which can enhance the dissipation of microwave.[3,19,20] Additionally, the small amount of P in Ni-Fe-P coating improves the synthetic magnetic properties of coating by increasing the resistivity value (ρ).[21] Meanwhile, compared with the metal powder reported in the literatures,[22,23] the Ni-Fe-P coating have a lower real part of complex permittivity, which increases the reflection coefficient for microwave absorption. Moreover, it has been shown that the absorption materials coated or embedded with metal nano-particles exhibits excellent microwave absorption performance, owing to the strong electric interfacial polarizations and high saturation magnetization.[24-29] Therefore, in this study, Ni-Fe-P coating was electroplated on the surface of CF to fabricate composite materials (CF@Ni-Fe-P), as illustrated in Fig. 1. It is expected that these novel CF@Ni-Fe-P materials could be the suitable candidates for the high-performance microwave absorption materials.

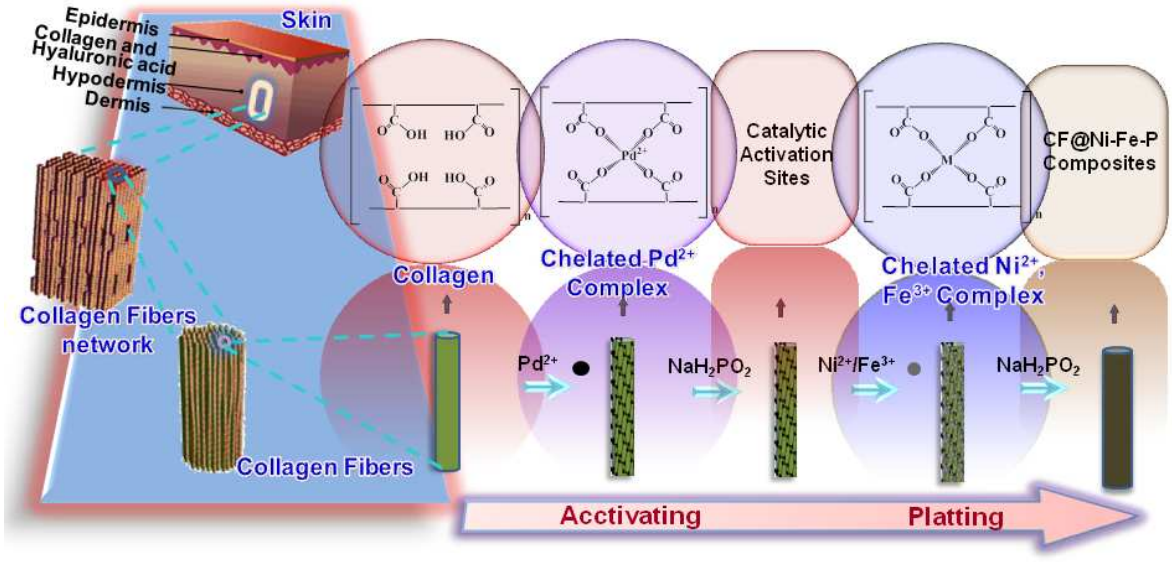

Fig. 1 Schematic diagram showing the preparation mechanism of the Ni-Fe bimetallic coating on CF.

Experimental

Materials synthesis

Firstly, the CF was prepared from cattle skin according to the procedures reported in our previous work.[30] Then, the obtained CF matrix was suspended into proper amount of distilled water with stirring. After the pH of mixture was lowered to 2.5 by formic acid, 4.0% (based on the weight of the CF) of glutaraldehyde solution was added into the mixture and stirring reacted at 298.0 K for 1.0 h.

Then, 1.0 g of gularadehyde crosslinked CF was activated by suspended in the mixture solution of 0.6 mmol/L of $PdCl_2$ and 0.6 mol/L of $NaH_2PO_2 \cdot H_2O$. After that, the pH and temperature were increased to 9.0 and 343.0 K, respectively. Then, the reaction was kept for 1.0 h under constant stirring. The main composition of eletroless plating bath was exhibited in Table 1.

Table 1. The composition of electroless plating bath.

Main Salts	Complexing Agent	Reducing Agent	Stabilizer	Buffer Agent
$NiSO_4 \cdot 6H_2O$	NH_2CH_2COOH			
0.5×10^{-1} mol/L	2.5×10^{-1} mol/L	NaH_2PO_2	NH_2CH_2COOH	H_3BO_3
		0.4 mol/L	0.5 mol/L	0.1×10^{-2} mol/L
$FeSO_4 \cdot 7H_2O$	$NaKC_4H_4O_6$			
0.5×10^{-1} mol/L	3.5×10^{-1} mol/L			

Lastly, the CF@Ni-Fe-P composites were fully washed with distilled water and dried in vacuum at 303.0 K for 24.0 h. The CF@Ni-Fe-P composites obtained with different volume (10.0 mL, 25.0 mL, 50.0 mL) of electronic plating bath were noted as CF@Ni-Fe-P-10, CF@Ni-Fe-P-25 and CF@Ni-Fe-P-50 respectively.

Characterization

The surface morphologies of CF@Ni-Fe-P composites were observed by Field Emission Scanning Electron Microscopy (FESEM, Hitachi 4700, Japan). The X-ray diffraction pattern of CF@Ni-Fe-P was recorded using a Cu-K a wide-angle X-ray diffraction pattern diffractometer (XRD, Philips X'Pert Pro-MPD, Netherlands). X-Ray photoelectron spectra (XPS, Shimadzu ESCA-850, Japan) of CF@Ni-Fe-P was recorded by employing Mg-K a X-radiation (hv ¼ 1253.6 eV) and a pass energy of 31.5 eV. Peaks from all the high-resolution core spectra were fitted with XPS PEAK 4.1 software, using mixed Gaussian-Lorentzian functions. The TEM characterization was performed by using Tecnai G 2 F20 (TEM, FEI, Netherlands) operating at 200 kV. Magnetization measurements of theses samples were performed on a Quantum Design MPMS-XL5 SQUID magnetometer. CF@Ni-Fe-P composites were pressed into a toroidal shaped mold (φ_{out}=7.0 mm, φ_{in}=3.0 mm) for the measurements of complex permittivity ($\varepsilon_r=\varepsilon'-j\varepsilon''$) and complex permeability ($\mu_r=\mu'-j\mu''$) by using a vector network analyzer (VNA, Agilent E8363B, Agilent, Santa Clara, CA) in the frequency range of 2.0~18.0 GHz. The reflection loss values of microwave (RL) were calculated by using Matlab software (a registered trademark of The Math Work, Inc.) based on the measurements of complex permittivity and complex permeability using transmission line theory.

Results and discussion

Preparation of CF@Ni-Fe-P composites

In present investigation, the thermal denatured temperature of raw CF is about 333.0 K, but it was greatly increased to about 358.0 K after glutaraldehyde crosslinked, meeting the demands of electroless plating.[31,32] The succeeding surface sensitization and activation treatment with $PdCl_2$ result in the formation of palladium particle, which act as the catalytic activation sites for the reduction of Ni^{2+} and Fe^{3+} during electroless plating. Moreover, the CF 3D network is conducive to catch the Ni-Fe-P coating and Pd strongly, due to the fact that the groups of carboxyl (-COOH) and amino(-NH_2) of CF are capable of chelating with some metal ions, such as Fe^{3+}, Ni^{2+}, Pd^{2+}, Cr^{3+}, Al^{3+}, ect.[28,33,34]

Characteristics of CF@Ni-Fe-P composites

At presented in Fig. 2, SEM images indicated that the surfaces of CF@Ni-Fe-P keep their initial ordered fibrous state of CF with approximately 10.0~20.0 μm in diameter, which is assigned for the diameter of the bundle for natural CF. It deserved to note that the fine hierarchy of CF@Ni-Fe-P structure is masked with increasing the volume of electroless plating bath, especially for the CF@Ni-Fe-P-50 (d). Therefore, the thickness of Ni-Fe-P coating can be easily adjusted by varying the volume of electroless plating bath.

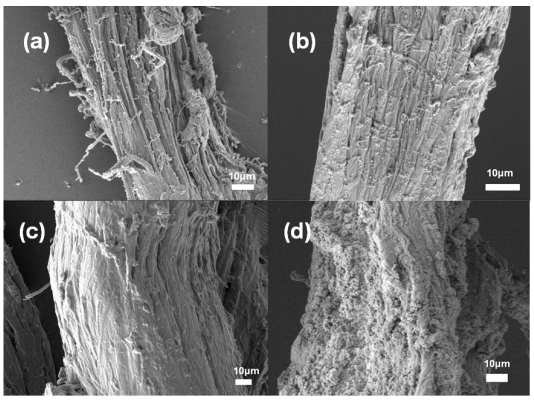

Fig. 2 Field emission electron microscopy (FE-SEM) images of CF (a), CF@Ni-Fe-P-10 (b), CF@Ni-Fe-P-25 (c), CF@Ni-Fe-P-50.

To verify the Ni-Fe-P coating on the CF, the typical X-ray diffraction (XRD) patterns of CF@Ni-Fe-P-10 composite is presented in Fig. 3. It can be seen that the XRD spectra of CF@Ni-Fe-P-10 composite exhibits a broad peak around at 2θ=23.0º, which is attributed to the amorphous polymer phase of CF.[9] As expected, there is another broad peak around at 2θ=45.0º, which is attributed to the amorphous structure of Ni-Fe-P.[35] In addition, there are two weak crystalline peaks. The peak around at 2θ=35.0º is attributed to the Ni hydroxides, and the other peak around at 2θ=60.0º is attributed to the Fe hydroxides.

In order to evaluate the electronic state of the as-prepared Ni-

Fe-P coating, the CF@Ni-Fe-P-10 composite is determined by X-ray photoelectron spectra (XPS), as shown in Fig. 4. From the Ni 2p energy lever in Fig. 4a, it can be seen that almost Ni species are presented in metallic state around 855.7 eV and 873.4 eV, which are attributed to the Ni in the Ni-Fe-P coating. Meanwhile, there are two satellite peaks around 861.7 eV and 879.7 eV, which are attributed to the Ni^{2+} and metallic Ni, respectively.[33] From Fe 2p energy lever in Fig. 4b, the Fe species are presented in both the metallic state and the oxidized state (Fe^{3+}) around at 712.0 eV and 723.0 eV, respectively.[36,37] Meanwhile, there are two peaks for the O 1s species in Fig. 4c. The peak at 532.1 eV is attributed to the original O=C groups of CF, and the other around at 530.8 eV is attributed to the Ni hydroxides and Fe hydroxides, such as $Ni(OH)_2$ and $Fe_2Ni(OH)$.[38] However, the N 1s energy lever appears single peak around at 400.0eV in Fig. 4d, which is attributed to the O=C–N of CF.

The CF@Ni-Fe-P-25 composite was observed by transmission electron microscopy (TEM). As shown in Fig. 5, CF is indeed coated by a highly dense layer with the thickness of 50.0~100.0 nm. Moreover, energy dispersive X-ray (EDX) analysis indicates that the coating layer consists of Ni, Fe and P. These results confirm the successful coating of Ni-Fe-P on the surface of CF.

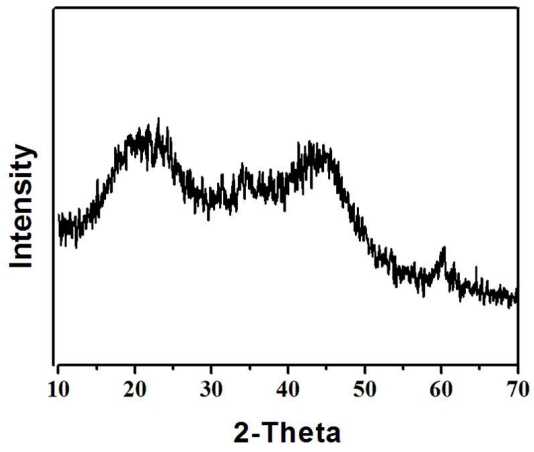

Fig. 3 X-Ray diffraction (XRD) pattern of the CF@Ni-Fe-P-10.

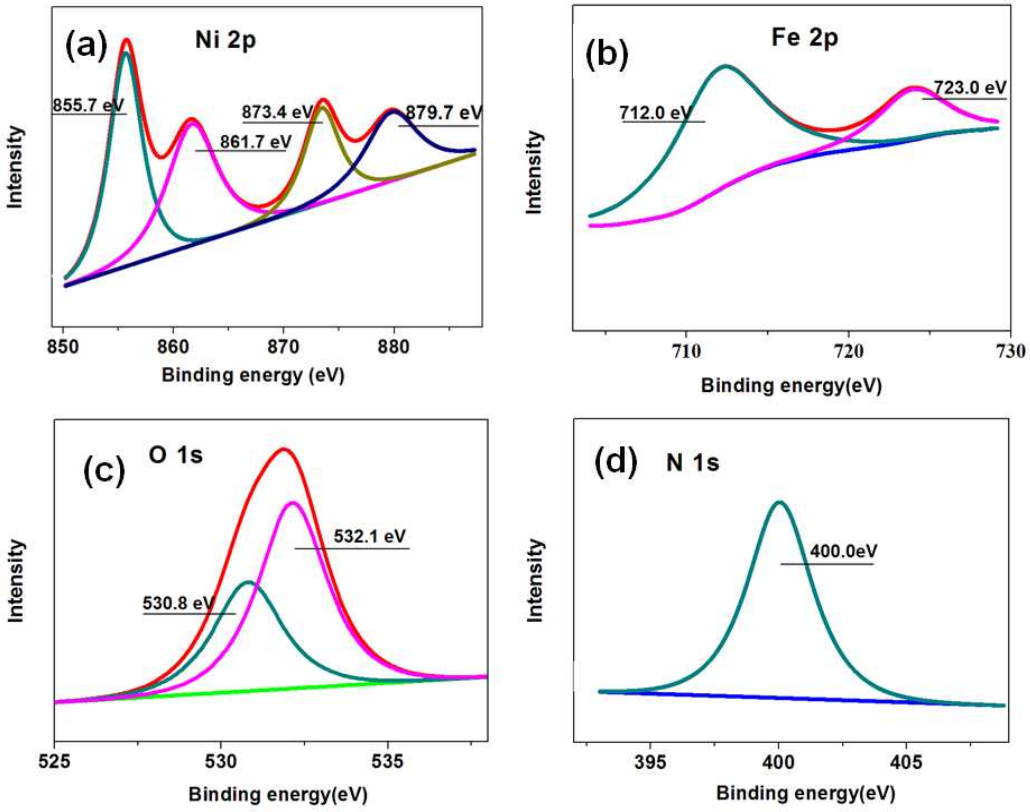

Fig. 4 Ni 2p (a), Fe 2p (b), O 1s (c) and N 1s (d) energy levels X-ray photoelectron spectra (XPS) for the CF@Ni-Fe-P-10.

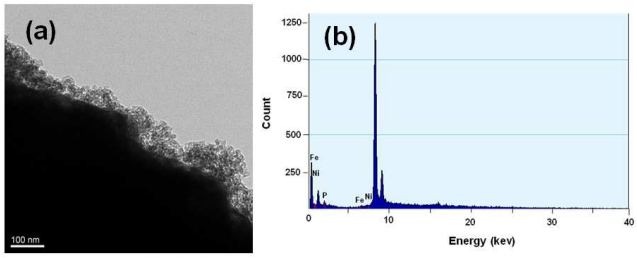

Fig. 5 Transmission electron microscopy (TEM) image of the CF@Ni-Fe-P-25 composite (a) and energy dispersive X-ray (EDX) spectra of the coating layer (b).

Microwave absorbing abilities of CF@Ni-Fe-P fibrous composites

To reveal the microwave absorption performance of fibrous CF@Ni-Fe-P composites, the reflection-loss (RL) values of CF and CF@Ni-Fe-P composites are calculated using the relative complex permeability and complex permittivity at a given thickness of layer according to the transmit theory, which is summarized as the following equations: [39]

$$RL = 20\log\left[\left(Z_{in} - Z_0\right)/\left(Z_{in} + Z_0\right)\right] \quad (1)$$

$$Z_{in} = Z_0\sqrt{\mu_r/\varepsilon_r}\tanh\left[j\left(2\pi/c\right)\sqrt{\mu_r\varepsilon_r}fd\right] \quad (2),$$

where Z_{in} is the input impedance of absorber. Z_0 is the impedance of air. f is the frequency of microwave. d is the thickness of microwave absorbing materials. c is the velocity of light. μ_r and ε_r are the complex permeability and complex permittivity of the CF@Ni-Fe-P, which are tested on a network analyzer in the frequency range of 2.0~18.0 GHz.

Concerning the intrinsic electric conductivity, biological composites often do not exhibit the desired microwave absorbing properties. Fig. 6a has shown that the CF nearly have no microwave absorbing ability over the whole frequency range of 2.0~18.0 GHz (RL≈-3.0 dB). However, when the CF is coated by the Ni-Fe-P coating, the RL values of these CF@Ni-Fe-P composites show a dramatic increase with 2.4 mm of the thickness T. In case of CF@Ni-Fe-P-10 with low coated degree of Ni-Fe-P coating, its RL values exceeding -10.0 dB can cover the frequency range from 13.0 GHz to 18.0 GHz and its maximum RL value reaches up to about -24.0 dB at 17.0 GHz. When the volume of electroless plating bath was increased, the maximum RL value of CF@Ni-Fe-P-25 reaches up to -26.0 dB and the frequency band of RL values exceeding -10.0 dB become broader from 11.0 GHz to 18.0 GHz. However, when the volume of electroless plating bath was further increased, the RL values of CF@Ni-Fe-P are decreased instead and the frequency range of RL values exceeding -10.0 dB become narrow. Therefore, compared with the pure CF, the CF@Ni-Fe-P composites possess excellent microwave absorption property, especially the CF@Ni-Fe-P-25 composite.

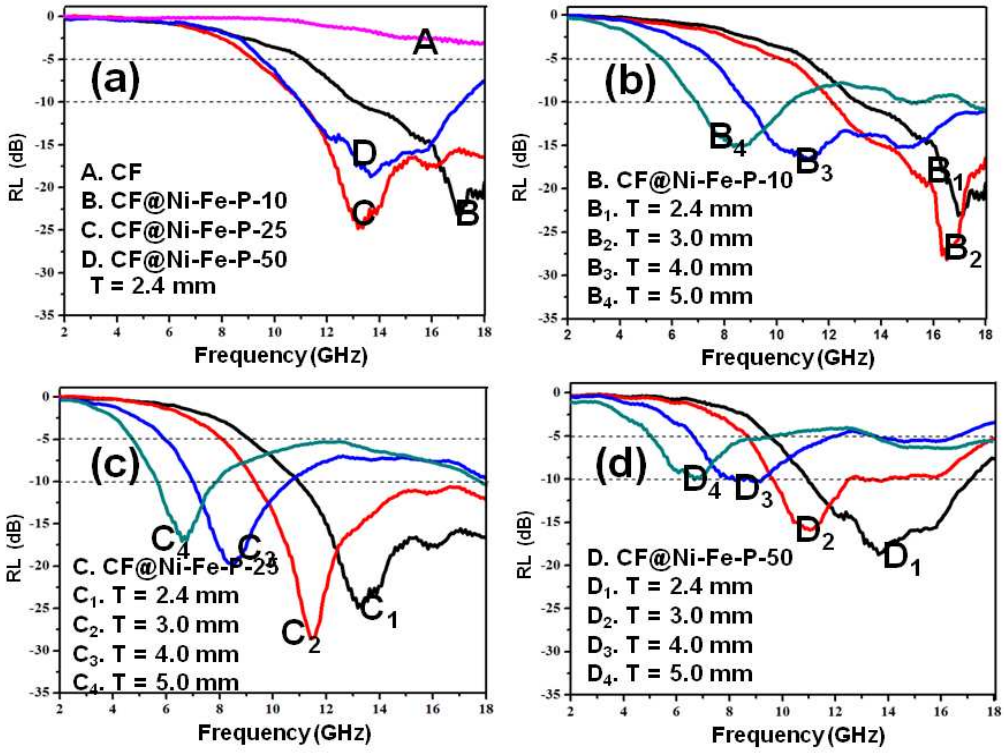

Fig. 6 Microwave reflection losses (RL) comparison of the microwave reflection losses (RL) of CF and different CF@Ni-Fe-P composites with thickness T=2.4 mm (a), and CF@Ni-Fe-P-10 (b), CF@Ni-Fe-P-25 (c), CF@Ni-Fe-P-50 (d) with different thickness from 2.4 mm to 5.0 mm.

It is well known that the thickness of absorption material is one of the crucial parameters that affect the absorbing intensity and frequency range. Therefore, we further established the relationship of RL values of these CF@Ni-Fe-P with different thicknesses of 2.4 mm, 3.0 mm, 4.0 mm, and 5.0 mm, as shown in Fig. 6b to Fig. 6d. The microwave absorption ability in the S-band (2.0~4.0 GHz) and C-band (4.0~8.0 GHz) of the common microwave absorption materials is usually very weak (less than -5.0 dB), which is not suitable for the wide-band microwave absorption application. However, the RL values exceeding -5.0 dB of CF@Ni-Fe-P-10 and CF@Ni-Fe-P-25 composites cover the whole X-band and Ku-band (8.0~18.0 GHz) and some part of C-band (4.6~8.0 GHz) at the thickness of 5.0 mm in Fig. 6b and Fig. 6c. In the case of CF@Ni-Fe-P-25, its RL values exceeding -10.0 dB can cover the whole X-band and Ku-band and some part of C-band (5.5~8.0 GHz), and its maximum RL value is -31.0 dB, when the thickness changes from 2.4 mm to 5.0 mm, as shown in Fig. 6c. Moreover, when the thickness of CF@Ni-Fe-P-25 is increased to 3.0 mm, the absorption frequency band almost covers the whole X-band and Ku-band (9.3~18.0 GHz), which is critically important for both commercial and military defensive purposes. For the CF@Ni-Fe-P-50, as shown in Fig. 6d, its microwave absorbing intensity is reduced when the thickness is increased from 2.4 mm to 5.0 mm, and its maximum RL value is about -20.0 dB at the thickness of 2.4 mm. And its RL values exceeding -10.0 dB can still cover from 10.5 GHz to 17.5 GHz, when the thickness is 2.4 mm. Therefore, CF@Ni-Fe-P shows promise for use as low-cost and highly efficient microwave absorption material.

Microwave absorption mechanism of CF@Ni-Fe-P composites

To reveal the possible absorbing mechanism of CF@Ni-Fe-P composites, the complex permittivity (ε′ and ε″) and complex permeability (μ′ and μ″) of the CF and CF@Ni-Fe-P were measured using a vector network analyzer in the frequency range of 2.0~18.0 GHz, independently. Fig. 7 shows the variations of the electromagnetic parameter (complex permittivity and complex permeability), dielectric loss ($\tan\delta_d$) and magnetic loss ($\tan\delta_m$) in the frequency of 2.0~18.0 GHz. The dielectric loss ($\tan\delta_d$) and magnetic loss ($\tan\delta_m$) are calculated according to the following equations:

$$\tan\delta_d = \varepsilon''/\varepsilon', \tan\delta_m = \mu''/\mu' \quad (3)$$

In general, the complex permittivity results from orientation polarization, atomic polarization and electronic polarization.[2] As shown in Fig. 7a, all CF@Ni-Fe-P composites show high dielectric constant (ε′≈3.5~8.0), which is attributed to the high values of capacitance resulting from space charge polarization between adjacent conductive bulks. In Fig. 7b, the ε″ of CF@Ni-Fe-P-10 is between 1.5 and 2.0, and appears a weak peak at the frequency of 16.0~18.0 GHz, which tendency is in concordance with its RL. When the volume of electroless plating bath was increased to 25.0 mL, the ε″ of CF@Ni-Fe-P-25 is further increased (ε″≈2.3~2.6), and exhibits a peak between 12.0 GHz and 16.0 GHz. This increase should be originated from the enhancement of orientation polarization, atomic polarization and electronic polarization, especially the resonance in low-frequency caused by vacancies and pores of CF@Ni-Fe-P hierarchical structures.[40] However, the ε″ of CF@Ni-Fe-P-50 is decreased drastically to ε″≈1.5~2.3 with a weak fluctuation between 12.0 GHz and 16.0 GHz, which may be ascribed to skin depth of Ni-Fe-P coating.[20] In addition, it can be observed from Fig. 7c that $\tan\delta_d$ of CF is 0.1~0.3 owing to the poor conductivity of CF. When CF was coated with Ni-Fe-P layer, the corresponding $\tan\delta_d$ of CF@Ni-Fe-P is increased along with the increase of electroless plating volume from 10.0 to 25.0 mL, and then, decreased with the further increase of electroless plating volume to 50.0 mL. Indeed, these results demonstrate that the CF@Ni-Fe-P-25 owns the highest dielectric loss for microwave in the frequency of 2.0~18.0 GHz. This phenomenon suggests that as the conductivity of CF@Ni-Fe-P increases to some extent, the dielectric loss of CF@Ni-Fe-P decreases instead of continually increasing, which is attributed to the skin depth decreases with increasing conductivity. Therefore, the thickness of Ni-Fe-P coating should be properly controlled to obtain higher ε″ for the purpose of enhancing dielectric loss of CF@Ni-Fe-P composites.

In Fig. 7d and Fig. 7e, the date of complex permeability ($\mu_r = \mu' - j\mu''$) for CF@-Ni-Fe-P were 1.0~1.3. The μ′ and μ″ of CF@Ni-Fe-P show a complex behaviour due to difference of magnetic properties of Ni-Fe-P bulks coated on CF. In Fig. 7f, $\tan\delta_m$ of CF is around zero owing to its non-magnetic property. For the CF@Ni-Fe-P, the corresponding $\tan\delta_m$ is also increased along with the increase of electroless plating volume from 10.0 to 25.0 mL, and then, decrease with further increasing electroless plating volume to 50.0 mL. In general, the magnetic loss derives mainly from the magnetic hysteresis, domain wall resonance, natural resonance and eddy current loss for a magnetic materials.[41] Among of these, the irreversible magnetization can generate hysteresis loss, and domain wall resonance often occurs in low frequency.[2,16] Hence, the magnetic loss of as prepared CF@Ni-Fe-P composites is mainly come from the natural resonance and eddy current loss.[29]

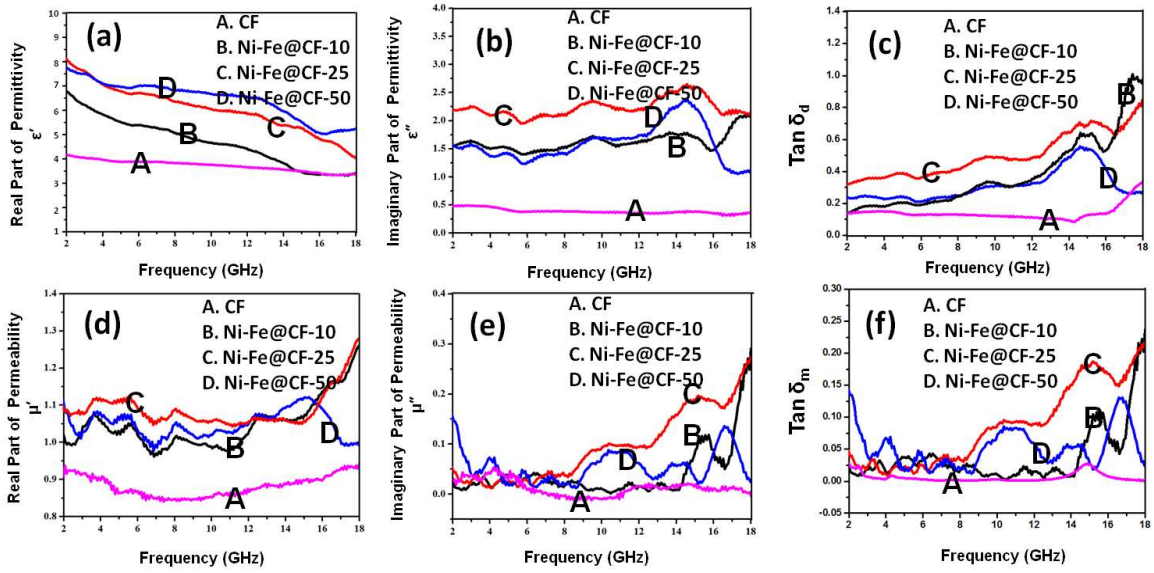

Fig. 7 Variations of real part of complex permittivity (a), imaginary part of complex permittivity (b), the dielectric loss tanδ_d (c), real part of complex permeability (d), imaginary part of complex permeability (e), and magnetic loss tanδ_m (f) of the CF, CF@Ni-Fe-P-10, CF@Ni-Fe-P-25 and CF@Ni-Fe-P-50 in the frequency of 2.0~18.0 GHz.

To investigate the magnetic properties of CF@Ni-Fe-P, the values of saturation magnetization (Ms) and the coercivity (Hc) at room temperature by Vibrating Sample Magnetometer (VSM). In Fig. 8a, the magnetic properties, Ms and Hc, derived from the hysteresis loops were listed in Fig. 8a, ESI†. When the volume of electroless plating bath was increased from 10.0 mL to 25.0 mL, the Ms values of CF@Ni-Fe-P are increased from 28.0 emu/g to 188.8 emu/g , while the Hc values are decreased from 87.5 Oe to 51.2 Oe. However, the Ms value of Ni-Fe@CF-50 is decreased and Hc value of Ni-Fe@CF-50 is increased. This might due to the facts that the hierarchical structure of CF is masked by Ni-Fe-P coating and lager Ni-Fe-P bulks accumulated on the surface of CF.[29,42,43]

The other magnetic dissipation of the ferromagnetic absorber is usually caused by eddy current effect, and the eddy current loss can be evaluated by the following equation:[13,24]

$$\mu'' \approx 2\pi\mu_0 (\mu')^2 \sigma d f / 3 \quad (4),$$

where σ (S cm^{-1}) is the electrical conductivity and μ_0 (H m^{-1}) is the permeability in vacuum. If the reflection loss is resulted from the eddy current loss, the values of C_0 ($C_0=\mu''(\mu')^{-2} f^{-1}$) are constant when the frequency is changing. Fig. 8b is the variations of C_0 ($C_0=\mu''(\mu')^{-2}f^{-1}$) of frequency for CF@Ni-Fe-P-25. It can be observed that the value of C_0 is almost constant in the frequency ranges from 9.0 GHz to 11.5 GHz. This result implies that the CF@Ni-Fe-P have a significant eddy current loss effect for the microwave energy.

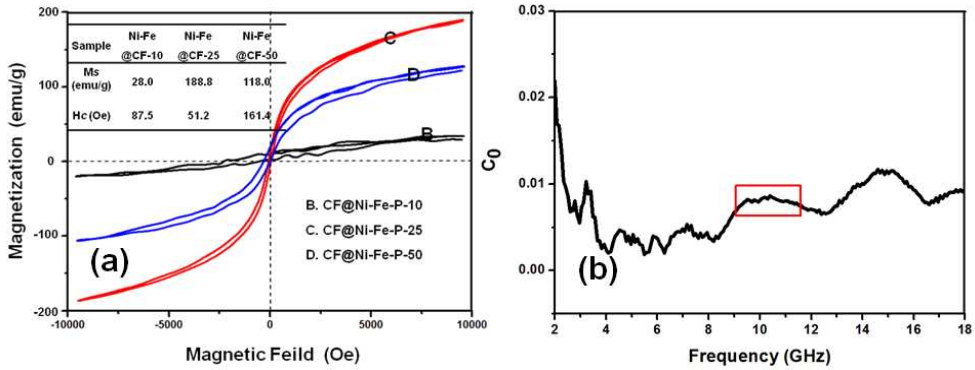

Fig. 8 Magnetic hysteresis loops of CF@Ni-Fe-P-10, CF@Ni-Fe-P-25, CF@Ni-Fe-P-50, inset table of the Ms and Hc values of CF@Ni-Fe-P composites (a) and variations of C_0 ($C_0 = \mu''(\mu')^{-2}f^{-1}$) for CF@Ni-Fe-P-25 (b) in the frequency of 2.0~18.0 GHz.

Finally, we measured the attenuation constants of native CF and CF@Ni-Fe-P. The attenuation constant is calculated according the following equation:[44]

$$\alpha = \frac{\sqrt{2}\pi f}{c} \times \sqrt{(\mu''\varepsilon''-\mu'\varepsilon')+\sqrt{(\mu''\varepsilon''-\mu'\varepsilon')^2+(\mu''\varepsilon'+\mu'\varepsilon'')^2}} \quad (5),$$

where f is the frequency, c is the speed of light. As shown in Fig. 9, the attenuation constant of CF is 0.1~0.5 in the frequency of 2.0~18.0 GHz. After the coating of Ni-Fe-P active composites, the calculated attenuation constants were found to increase significantly. For example, the attenuation constant of CF@Ni-Fe-25 is 0.7~1.2 in the frequency of 2.0~18.0 GHz. Indeed, these results demonstrate that the coating of Ni-Fe-P on CF is essential for achieving high-performance microwave absorption ability, due to the improved dielectric loss and magnetic loss for microwave absorption in the frequency 2.0~18.0 GHz.

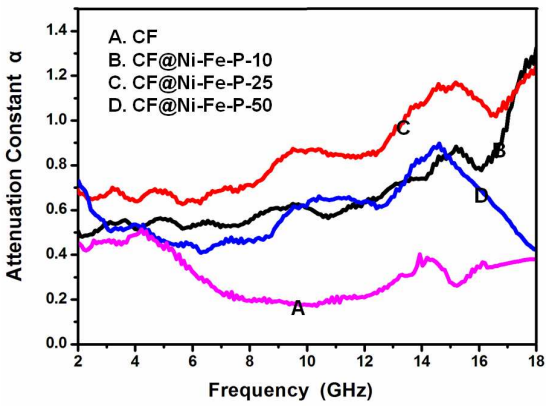

Fig. 9 Variations of attenuation constant for CF and CF@Ni-Fe-P composites in the frequency of 2.0~18.0 GHz.

Conclusions

In summary, we demonstrated the design and fabrication of CF@Ni-Fe-P composites using natural skin collagen fiber as the matrix. The as-prepared CF@Ni-Fe-P composites exhibit an excellent microwave absorption performance in the whole X-band and Ku-band. The present work presents a new approach for developing, lightweight, low-cost and wide-band microwave absorbing materials based on natural biomass.

Acknowledgements

This work is supported by the Key Program of the National Natural Science Foundation of China (21176161) and the New Century Talents Support Program (NCET-11-D358). We thank Junling Guo in the Department of Chemical and Biomolecular Engineering, The University of Melbourne, for the helpful discussion and revision of manuscript. We also thank Prof. Liang Chen in the Engineering Research Center of Stealth Materials and Technology for the microwave adsorption measurements.

Notes and references

a. Department of Leather Chemistry and Engineering, Sichuan University, Chengdu, China. E-mail: xpliao@scu.edu.cn; Fax: +86-28-85400356;Tel: +86-28-85400382

b. National Engineering Laboratory for Clean Technology of Leather Manufacture, Sichuan University, Chengdu, P. R. China. E-mail: sibitannin@vip.163.com

***Corresponding Author**
Tel: +86-028-85400382; Fax: +86-028-85400356.
E-mail: xpliao@scu.edu.cn; shibi@scu.edu.cn.

1. Z. B. Li, B. Shen, Y. D. Deng, L. Liu and W. B. Hu, *J. Appl. Surf. Sci.*, 2009, **255**, 4542.
2. J. H. Liu, X. L. Zhang, S. M. Li and M. Yu, *J. Appl. Surf. Sci.*, 2011, **257**, 2383.
3. R. C. Che, L. M. Peng, X. F. Duan, Q. Chen and X. L. Liang, *J. Adv. Mater.*, 2004, **16**, 401.
4. J. C. Wang, C. S. Xiang, Q. Liu, Y. B. Pan and J. K. Guo, *J. Adv. Funct. Mater.*, 2008, **18**, 2995.
5. X. H. Guo, Y. H. Deng, D. Gu, R. C. Che and D. Y. Zhao, *J. Mater. Chem.*, 2009, **19**, 6706.
6. X. Bai, Y. H. Zhai and Y. Zhang, *J. Phys. Chem.*, 2011, **115**, 11673
7. K. Y. Park, J. H. Han, S. B. Lee, J. B. Kim, J. W. Yi and S. K. Lee, *J Comps. Sci. Technol.*, 2009, **69**, 1271.
8. Y. Y. Wang and X. L. Jing, *J. Polym. Advan. Technol.*, 2005, **16**, 344.
9. L. D. Liu, Y. P. Duan, L. X. Ma, S. H. Liu and Z. Yu, *J. Appl. Surf. Sci.*, 2010, **257**, 842.
10. R. F. Zhuo, H. T. Feng, J. T. Chen, D. Yan, J. J. Feng, H. J. Li, B. S. Geng, S. Cheng, X. Y. Xu and P. X. Yan, *J. Phys. Chem. C*, 2008, **112**, 11767.
11. M. S. Cao, W. L. Song, Z. L. Hou, B. Wen and J. Yuan, *J. Carbon*, 2010, **48**, 788.
12. M. N. Iqbal, M. F. B. A. Malek, S. H. Ronald, M. S. B. Mezan, K. M. Juni and R. Chat, *J. Prog. Electromagn. Res.*, 2012, **131**, 19.
13. J. L. Guo, X. L. Wang, X. L. Liao, W. H. Zhang and B. Shi, *J. Mater. Chem.*, 2012, **22**, 11933.
14. J. L. Guo, X. L. Wang, X. L. Liao, W. H. Zhang and B. Shi, *J. Phys. Chem. C*, 2012, **116**, 8188.
15. J. L. Guo, X. L. Liao, W. H. Zhang and B. Shi, *J. AM Leather Chem.*, 2012, **107**, 205.
16. M. Z. Wu, H. H. He, Z. S. Zhao and X. Yao, *J. Phys. D: Appl. Phys.*, 2000, **33**, 2398.
17. A.F. Shmeckenbecher, *J. Electrochem. Soc.*, 1966, **113**,778.
18. W. O. Freitag, J. S. Mathias and G. D. Guilio, *J. Electrochem. Soc.*, 1964, **111**,35.
19. X. G. Liu, B. Li, D. Y. Geng, W. B. Cui, F. Yang, Z. G. Xie, D. J. Kang and Z. D. Zhang, *J. Carbon*, 2009, **47**, 470.
20. G. Q. Wang, L. F. Wang, Y. L. Gan and W. Lu, *J. Appl. Surf. Sci.*, 2013, **276**, 744.
21. A. F. Schmeckenbecher, *J. Plating*, 1971, **58**, 905.
22. X. A. Li, X. J. Han and Y. J. Tan , *J. Alloys Compd.*, 2008, **464**, 352.
23. P. Chen, R. X. Wu, T. N. Zhao, F. Yang and J. Q. Xiao, *J. Phys. D: Appl. Phys.*, 2005, **38**, 2302.
24. J. H. Zhu, S. Y. Wei, N. Haldolaarachchige, D. P. Young and Z. H. Guo, *J. Phys. Chem. C*, 2011, **115**, 15304.
25. Z. G. An, S. L. Pan and J. J. Zhang, *J. Phys. Chem. C*, 2009, **113**, 2715.
26. A. Ohlan, K. Singh, A. Chandra and S. K. Dhawan, *J. Acs Appl. Mater. Inter.*, 2010, **2**, 927.
27. G. V. Ramesh, S. Porel and T. P. Radhakrishnan. *J. Chem. Soc. Rev.*, 2009, **38**, 2646.
28. E. Royston, A. Ghosh, P. Kofinas, M. T. Harris and J. N. Culver. *J. Langm.*, 2008, **24**, 906.

29. S. F. Zhou, Q. X. Zhang, H. Liu, X. Gong and J. Huang, *J. Mater. Chem. Phys.*, 2012, **134**, 224.
30. Z. B. Lu, X. P. Liao and B. Shi, *J. Society of Leather Technologists and Chemistry (in chinese)*, 2003, **87**,173.
31. Y. H. Zeng, X. Sun, X. P. Liao and B. Shi, *J. Leather Science and Engineering (in chinese)*, 2007, **17**, 16.
32. D. P. Speer, M. Chvapil, C. D. Eskelson and J. Ulreich, *J. Biomed. Mater. Res.*, 1980, **14**, 753.
33. A. D. Covington, *J. Chem. Soc.,* 1997, **26**, 111.
34. D. H. Deng, H. Wu, X. P. Liao and B. Shi, *J. Microporous Mesoporous Mater.*, 2008, **116**, 705.
35. X. H. Yan, J. Q. Sun, Y. W. Wang and J. F. Yang, *J. Mol. Catal. A: Chem.*, 2006, **252**, 17.
36. N. Li and Z. M. Tu, In electroless plating technology, 2nd, *Beijing*, 2004, pp. 176-178.
37. C. Q. Li, X. F. Zhang, W. N. Wang, X. G. Zhu and X. L. Dong, *J. Mater. Eng.,* 2006, 46.
38. E. Royston, A. Ghosh, P. Kofinas, M. T. Harris and J. N. Culver, *J. Langm.*, 2008, **24**, 906.
39. P. A. Rizzi, Microwave engineering: passive circuits. *Prentice Hall: Englewood Cliffs, NJ*, 1988, pp. 189-190.
40. A. Verma, A. K. Saxena and D. C. Dube, *J. Magn. Magn. Mater.*, 2003, **263**, 228.
41. X. L. Zhang, J. H. Liu and S. M. Li, *J. Mater. Lett.*, 2009, **63**, 1907.
42. S. S. Kim, S. T. Kim, J. M. Ahn and K. H. Kim, *J. Magn. Magn. Mater.*, 2004, **271**, 39.
43. S. Maensiri, C. Masingboon, B. Boonchom and S. Seraphin, *J. Scripta Mater.*, 2007, **56**, 797.
44. B. S. Zhang, Y. Feng, J. Xiong, Y. Yi and H. X. Lu, *J. Magn.*, 2006, **42**, 1778.